Bulletin of Biological and Allied Sciences Research
***ISSN:* 2521-0092**
www.bbasr.org
DOI: https://doi.org/10.54112/bbasr.v2023i1.54
*Bull. Biol. All. Sci. Res., Volume, **8**: 54*

Original Research Article

HYDROLOGICAL MODELING AND WATERSHED ANALYSIS OF SWAT RIVER BASIN BY USING HBV LIGHT MODEL AND ARC GIS

ISLAM A, AKRAM W*, NARMEEN R

College of Earth and Environmental sciences University of the Punjab, P.O.Box 54590,Lahore , Pakistan
**Correspondence author email address: wasiminayat19111@gmail.com*

(Received, 21th February 2023, Revised 10th December 2023, Published 13th December 2023)

Abstract *Climate change is a pivotal global phenomenon, particularly impactful in nations like Pakistan. This study delves into the myriad factors driving climate change, specifically focusing on its profound effects on economically vulnerable countries heavily reliant on natural resources for water. Utilizing historical climatic and discharge data from the Swat River, located within the Khyber Pakhtunkhwa province, the research employs temperature, precipitation, and discharge data to scrutinize changes in the KALAM basin at a regional level. Situated between 34° and 36° N latitude and 71° to 72° E longitude, the Swat River Basin relies heavily on glacier snowmelt. The HBV model and GIS techniques are harnessed to dissect climate variations within the KALAM Basin. GIS aids in mapping the study area and visualizing temperature fluctuations in the basin. The basic HBV rainfall-runoff model undergoes automatic calibration using a straightforward yet effective method, providing satisfactory results during the 1981-2000 calibration and 2001-2010 validation periods. Noteworthy findings include the HBV-light model's adeptness at simulating stream flow and snowmelt in the snow-fed basin. However, the study emphasizes the substantial impact of parameter set values on the model's performance, highlighting the challenge of selecting an ideal parameter configuration. Sensitivity tests underscore the significant influence of climate change, specifically temperature increases, on stream flow across yearly, seasonal, and snowmelt contributions. Employing geographic information systems (GIS) alongside a digital elevation model proves instrumental in managing and analyzing water resources, aiding in watershed delineation—a crucial step in hydrological modeling. GIS, particularly the Arc Hydro tool, is valuable for determining grid directions in catchment areas, drainage lines, and flow accumulation. The research underscores the need for comprehensive scientific exploration to address knowledge gaps and enhance understanding of the applications of the HBV light model in the context of climate variations, particularly concerning water resources.*

*[Citation: Islam, A., Akram, W., Narmeen, R. (2023). Hydrological modeling and watershed analysis of Swat river basin by using HBV light model and ARC GIS. Bull. Biol. All. Sci. Res. **8**: 54. doi: https://doi.org/10.54112/bbasr.v2023i1.54]*
Keywords: *climate change; Kalam basin; hydrology modeling; grid; water resources*

Introduction

Water, a ubiquitous element in our natural surroundings, manifests in three states: liquid, solid, and vapor. Its accumulation forms lakes, rivers, and oceans, while in a solid state, it transforms into ice and snow, predominantly in polar and alpine regions. The hydrological cycle, intertwined with other natural cycles, is influenced by the moisture present in the air (Macauley, 2010). Substantial quantities of water are sequestered due to mineral composition in the Earth's core. Categorized by chemical and physical properties, water types include saline (found in oceans), freshwater (used domestically and industrially), and an intermediate type for agriculture. Notably, 97.5% is saline, with only 2.5% being freshwater, a meager 0.26% of which is crucial for ecosystem survival in lakes and rivers (Mishra, 2023). Water is essential for life and the hydrological cycle and is a cornerstone for economic development, agricultural growth, and industrial progress. Facing scarcity in numerous regions, assessing water availability and scarcity is paramount for future resource management. Drawing water budget maps becomes crucial for water resource management entities, particularly focusing on watershed origins where hydrological processes interact with weather, topography, geology, and land use, all influenced by human activities (Acreman, 1999). Water resources and management projects worldwide undergo intense transformations, gaining attention in tandem with food concerns, given agriculture's heavy reliance on water and its quality. Water scarcity is a global challenge, impacting regions differently and emphasizing water's indispensable role in sustaining life and environmental processes. Crucially, water is essential for various physiological and biochemical

reactions, including those within and outside cells, protein and enzyme reactions, solute movement, and energy production (Molden, 2013).

The surface water hydrology in Pakistan is primarily regulated by the Indus River, fed by its five principal tributaries: Kabul, Jhelum, Chenab, Ravi, and Sutlej. The Indus River system, shaped like a funnel, amalgamates numerous water resources into a single river flowing into Pakistan (Malik and Ashraf, 2021). It governs the flow of three western rivers—Indus, Jhelum, and Chenab—while receiving additional contributions from eastern rivers, Sutlej and Ravi, showcasing diversions from India through distinct stream flows (Malik and Ashraf, 2021). The flow in Pakistani rivers relies heavily on monsoons, snowmelt, and glacier thaw, excluding Jhelum, which also receives water during the summer monsoon. Annual calculations of both tributaries' average flow from different stations amount to 142 Million Acre Feet (MAF), with the Indus River contributing over 45% to this annual flow. Pakistan experiences low yearly rainfall, primarily during the monsoon season, with the concentration and bulk of rain being unpredictable and challenging for crop cultivation (Ahmed). The groundwater aquifers in the Indus Plain serve as a significant freshwater source, recharged by precipitation, river flows, canal system leakage, water from minor distributaries, waterways, and agricultural activities (Ahmed). This freshwater distribution, amounting to around 40 MAF, is facilitated through pumping systems and a network of major and minor distributaries, serving agricultural, industrial, and domestic purposes across Pakistan. With a population of 160 million reliant on agriculture, Pakistan is recognized as the world's largest agricultural country. The irrigation infrastructure in the Indus Basin, developed over the past 150 years, comprises three major reservoirs (Tarbela, Mangla, and Chashma), 16 barrages, 2 Headworks, 2 siphons, 12 inter-river link canals, 44 canal systems across provinces, and over 107,000 waterways totaling approximately 56,073 kilometers(Habib, 2004). The Indus River system annually supplies 180 billion cubic meters (bcm) of water to Pakistan, with 128 bcm directed to the distribution network(Habib, 2004). Rainfall contributes about 50 bcm annually, and groundwater adds another 50–60 bcm. Further development of 20 bcm in groundwater is feasible through coordinated surface and groundwater use and strategic planning at basin and local levels. Past issues of salt problems and waterlogging in the Indus Basin due to inadequate groundwater utilization have shifted to current challenges of saltwater intrusion, surface salinization, and groundwater mining due to excessive use (Singh, 2017).

Climate change has far-reaching global impacts, particularly on freshwater resources. Assessing variations in mean annual runoff serves as an initial step. Still, it's crucial to delve into changes in river flow regimes and the temporal dynamics of discharge, essential for ecosystems and human well-being (Soundharajan et al., 2016). Projections from climate models underscore uncertainties, impacting global agricultural productivity and presenting challenges in measuring the effects of climate-induced drought. Pakistan's climatology, ranging from temperate to subtropic regions, features distinct seasons, influencing agriculture dependent on the monsoon system and glacier melting. The country's susceptibility to climatic events necessitates continuous study and classification (Khan et al., 2010). Climate change disrupts freshwater resources, influencing the hydrological cycle, air quality, and crop production, emphasizing the importance of hydrological models for understanding climate-water interactions (Soundharajan et al., 2016).

The continuous escalation in greenhouse gas emissions has led to global warming, foreseeing significant climate changes by the century's end. This gas surge, largely attributed to human activities, has transformed the atmosphere's composition, increasing daily global temperature (Ahmadi Dehrashid et al., 2022). Projections indicate a potential temperature rise of 1.8-4.0°C. Human-induced shifts in atmospheric and oceanic circulation and alterations in the hydrologic cycle contribute to heightened climate events, including floods and cyclonic formations (Kaur). These changes impact large glaciers and snow masses, influencing average sea levels and coastal areas. Mountains, sensitive to temperature changes, experience altered weather patterns, affecting snow and glacier dynamics. Studying glaciers and mountain systems is crucial for understanding and managing future climatic events, utilizing past observations to mitigate present impacts(Ahmadi Dehrashid et al., 2022). Increased atmospheric water vapors, precipitation pattern shifts, extensive snow and ice melting, soil humidity variations, and increased overflow are consequences of temperature-induced alterations on a global scale. This temperature shift significantly influences the hydrological cycle's intensity and precipitation distribution, impacting snow and rainfall activities during winter and ultimately affecting seasonal patterns and long-term climate-induced vegetation changes (Kaur).

The Swat River Basin, spanning 14,039 km2 within the Hindu Kush Mountains, encompasses a diverse geography in northern Pakistan. Positioned between 34°20′N and 35°56′N, and 70°59′E and 72°47′E, the area ranges from 375 m to the highest point at 5920 meters above mean sea level, with an average altitude of 2180 m. Vegetation thrives between 800 m and 3,400 m. Local meteorology indicates an average annual precipitation of 375 mm to 1250 mm, concentrated mainly in two seasons—winter (January to March) with westerlies and summer (July to September) with monsoons. The Swat River significantly influences the local economy, hosting two interconnected hydroelectric power plants with a total capacity of approximately 123 MW, contributing

to the national grid. Another hydropower project associated with the river aids various industrial and agricultural initiatives (Ashraf et al., 2014)(Figure 1).

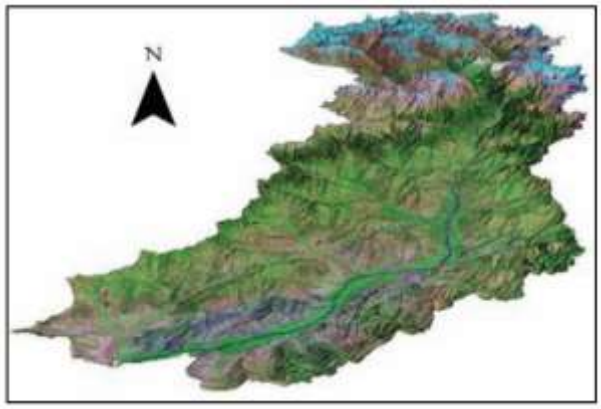

Figure 1: Landsat image of swat Basin

In the SWAT RIVER study, the HBV model was employed. It was designed to comprehensively capture hydrological conditions based on precipitation, discharge, and temperature. The choice of hydrological model is influenced by climate and terrain characteristics, ensuring suitability for basin modeling (Khorchani, 2016). The HBV model utilizes spatial data, including digital elevation models (DEM), soil data, climatic data, and land use/land cover maps. Meteorological data, such as precipitation, maximum and minimum temperatures, daylight hours, relative humidity, and wind speed, gathered by WAPDA, contribute to model output and aid in identifying future climatic predictions (Khorchani, 2016). The model's subdivision into sub-basins, watersheds, and sub-watersheds, as well as its differentiation between land use and land cover, enables the calculation of essential hydrological characteristics like evapotranspiration, surface runoff, maximum runoff rate, groundwater flow, and transmission losses (Khorchani, 2016) (Figure 2).

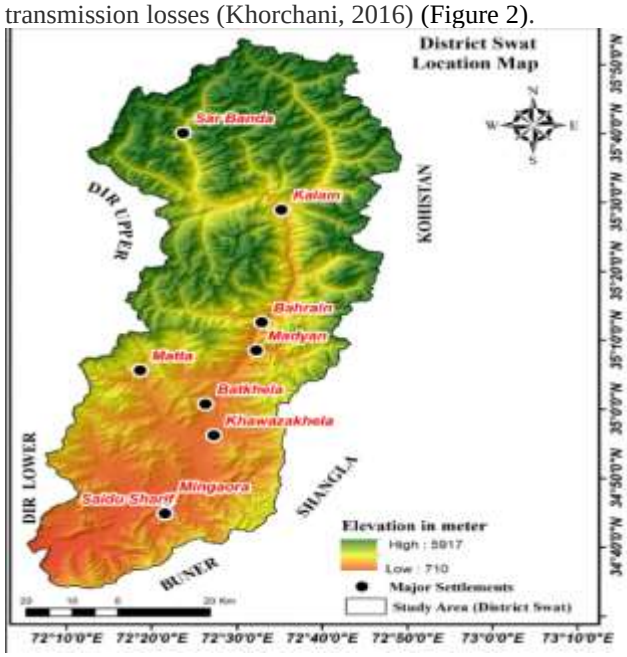

Figure 2: District swat location map

The research aimed to assess the HBV-light model's applicability to the Swat River Basin, outlining specific objectives. These included investigating the influence of various climatic factors on river flow, calculating annual and seasonal precipitation, maximum and minimum temperatures, and discharge at Kalam for the Swat Rive (Bizuneh et al., 2021) r. Additionally, the study sought to develop a GIS-based map for the specified area, compare calibration and validation results, and predict future climate change impacts. The overarching goal was to provide insights into the methodology applied throughout the research.

Material and Methodology

This study aims to observe the watershed analysis of Swat River using the HBV light model and ARC GIS effect of climate change on the rate of discharge, temperature, and rainfall. We used HBV light model for the hydrological modeling. It is a constant time model that runs on an annually time setup, and it is effective and accomplishes of endless simulation terminated elongated periods.

Data requirements

The data used in the modeling:

- Climatic data of thirty years (1981-2010) which is precipitation and temperature
- Discharge data of thirty years (1981-2010)
- Data on soil and land usage and cover
- Digital Elevation Model of the Swat River downloaded from SRTM website

Data collection

Thirty years of daily discharge data (1981-2010) and climatic data (precipitation, maximum and minimum temperature) were collected from WAPDA and Pakistan Metrological Department Lahore. The data is obtained for Swat river basin.

Methodology

The following methods and software are used:

HBV light model

The Hydrologiska Byrns Vattenavdelning (HBV) model, developed by the Swedish Meteorological and Hydrological Institute (SMHI) in the 1970s to support hydropower operations, has proven to be a globally robust and flexible tool for water resource problem-solving (Bouadila et al., 2020). With low data input requirements and manageable open model considerations, it has been widely used in diverse research projects. In West Africa, the HBV model demonstrated suitability for studying climate change effects and discharge simulation. Operating at daily time steps, the conceptual and lumped model includes diurnal rainfall and potential evapotranspiration (PET) data as input, addressing three primary hydrological processes: snowfall and sleet cover, soil moisture and dehydration, and groundwater and reaction mechanisms. The HBV-Light model used in snow-free catchments maintains the HBV model's structure with minor modifications, including the MAXBAS routing parameter and the incorporation of

a spin-up period instead of fixed initial states (Nonki et al., 2021).

Since its introduction, the HBV hydrological model has become a standard tool for hydrologists in the Nordic region and has been applied in over 50 countries for various purposes. Valuable in basins with limited data coverage or ungauged, it offers practical solutions with generalized parameter values. The model's adaptability extends to ungauged simulations, unlocking new possibilities in hydrological modeling (Nonki et al., 2021). Similar to many hydrological models, the HBV model employs the degree-day technique for snowmelt estimation. As a conceptual precipitation-runoff model, it simulates runoff processes in a catchment using precipitation and air temperature data. Catchment delineation is performed using the spatial analyst tool in Arc Map 10.0's hydrology extension (ESRI) (Vainu et al., 2015).

Metrological data

Daily precipitation, temperature, and discharge are the meteorological variables the HBV-Light model needs as input for this kind of analysis. This information was gathered from WAPDA.

Precipitation data

Data for at least 30 years is necessary to increase the potential of adding dry and wet years in the calibration and validation of rainfall-runoff modeling using the HBV model. Data on rainfall was gathered for the Swat Basin. The data collection period (1981–2010) was chosen with the availability of continuous observations in mind,

Temperature data

Maximum and lowest air temperature data were obtained from meteorological stations within the basin at a height of 2744 masl. The HBV model input for differentiating precipitation as snowfall or rainfall, computing snow melt, and calculating potential evapotranspiration uses the mean air temperature for each day.

Model Calibration

Calibration in the HBV-light model was conducted monthly using Swat's gauged discharge data provided by Wapda from 1981 to 2000. The data from 1981 to 1982 served to warm up and initialize the model variables, with no evaluation of model predictions during this period. The actual calibration utilized data from 1982 to 2000. Various factors within the HBV-light model account for diverse hydrological features across the watershed, and calibration of these process parameters is essential for accurate stream discharge replication. Since these parameters lack physical quantifiability, calibration becomes necessary, and previous studies employed various methods to estimate them. Harlin & Kung (1992) determined suitable parameter ranges by selecting minimum and maximum values from eight independent calibrations of two catchments (Bhattarai et al., 2018). Seibert (1999) estimated parameter values through 300,000 Monte Carlo simulations and three objective function scores. Booij (2005) identified ideal parameters by incorporating insights from previous scholars (Ali et al., 2018).

Criteria for model evaluation

NSE and R2 are the most popular efficiency standards for hydrological applications and flow comparisons when evaluating models (Moriasi et al., 2015). This study assessed the model's performance using the criteria mentioned above and mean difference error.

Nash-Sutcliffe efficiency (NSE) and Coefficient of determination (R2)

The efficiency E suggested by Nash and Sutcliffe (1970) is one minus the sum of the absolute squared differences between the predicted and observed values normalized by the variance of the observed values during the investigation period. This differs from the coefficient of determination (R2), defined as the squared value of the coefficient of correlation (McCuen et al., 2006).

Arc GIs

Geographic Information Systems (GIS) play a crucial role in water resource management, providing effective tools for storing, organizing, and visualizing geographic data. The applications of GIS in this field are diverse, including surface hydrologic and groundwater modeling, water supply and sewer system modeling, stormwater and nonpoint source pollution modeling for urban and agricultural areas. GIS is also utilized in transportation planning and engineering, facilitating various analytical activities. Despite challenges in obtaining funding and creating databases, organizations like the Lane Council of Governments in Eugene, Oregon, have been pioneers in GIS design, implementation, and management for decades, fostering multi-jurisdictional and multi-application approaches (Hanna et al., 1998).

Land use and land cover

The impact of changing land use and land cover on river basin hydrology is a significant concern in the context of global climate change. Selecting tools to assess these effects systematically is crucial, and GIS-based interfaces offer simplicity in connecting to tools for sensitivity, calibration, and uncertainty analysis. Evaluating the model's setup, performance, and physical representation of parameters involves various standards, ensuring a methodical approach (Moriasi et al., 2015). Utilizing Moderate Resolution Imaging Spectroradiometer Land Cover climatology with a spatial resolution of 500 x 500 m, the Swat basin exhibits diverse land cover types, including cropland (45.06%), grassland (29.41%), bare ground (12.44%), forests (6.55%), snow and ice (6.51%), and water bodies (0.02%) (Moriasi et al., 2015) (Figure 3 Table 1).

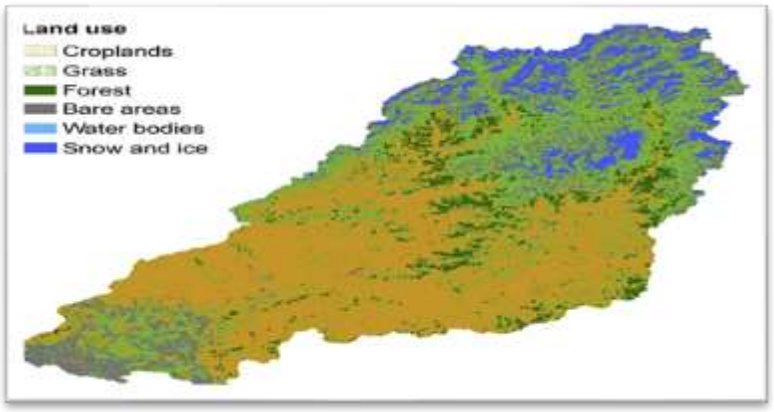

Figure 3: Land use of Swat

Table 1: Elevation zones of SWAT River

Elevation	Vegetation	Urban	Forest	Lake Area
570	0.00	0.00	0.00	0.00
1140	0.18	0.01	0.07	0.00
1709	0.07	0.00	0.13	0.00
2280	0.03	0.00	0.11	0.00
2850	0.03	0.00	0.08	0.00
3420	0.06	0.00	0.03	0.00
3990	0.10	0.00	0.00	0.01
4560	0.07	0.00	0.00	0.01
5130	0.01	0.00	0.00	0.00
5700	0.00	0.00	0.00	0.02

Study area

The Swat River, originating in Kalam and joining the Kabul River, flows south to Madyan through a narrow canyon, expanding into the Swat Valley and merging with the Panjkora River near Kalagay. The watershed spans from 34°00' to 35°56' north latitude and 70°59' to 72°47' east longitude. Munda Dam at Munda Headworks irrigates about 135,000 acres in the Peshawar Basin, serving a population of around 2,395,000 (Census-2017) (Anjum et al., 2016). With elevations between 1,800 and 3,400 meters, the region experiences visible vegetation and glaciers above 4,000 meters. Annual precipitation ranges from 375 mm to 1,250 mm, concentrated in winter and summer due to westerlies and monsoons, causing significant isolated precipitation during the summer (Anjum et al., 2016) (Figure 4 Table 2).

Table 2: Description of Study Area

Station	Kalam	Latitude	35 28 10	Length	240km(150mi)
River	Swat	Longitude	72 35 40	Source	Hindu Kush Mountain
Basin	Indus	Elevation of discharge	1921masl	Location	Charsadda
Catchment Area	2020km	Province	NWFP	Elevation of precipitation	7500 feet

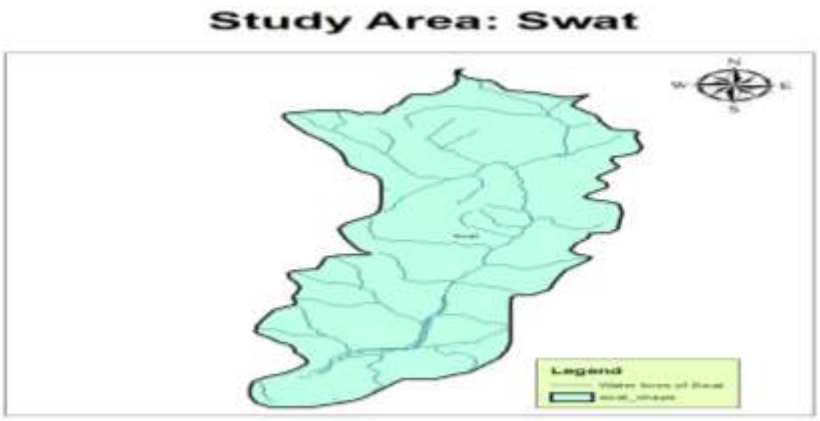

Figure 4: Study Area map of Swat

Topography

The Swat River, a primary tributary of the Kabul River, originates in the Kalam region, flowing south to Madyan through a narrow canyon. The Swat Valley expands downstream, turning westward near Kalagay, which merges with the river Panjkora's vast area. The watershed of the Swat River basin spans from 34°00' to 35°56' north latitude and 70°59' to 72°47' east longitude. Notable headworks in the basin include Amandara and Munda, with Munda Dam irrigating approximately 135,000 acres of land in the Peshawar Basin. The region sustains a population of about 2,395,000 (Census-2017)(Dawood et al., 2021). The elevation ranges between 1,800 and 3,400 meters, with visible vegetation and glaciers above 4,000 meters. Annual precipitation varies from 375 mm to 1,250 mm, concentrated in the winter and summer due to westerlies and monsoons. Summer monsoons, influenced by orographic lifting, lead to significant isolated precipitation events (Dawood et al., 2021).

Geology

The mountainous catchment area of the Swat River is predominantly sandy, constituting an average forest cover of 17%, varying from 5% in the lower Valley to 25% in the upper reaches. Agricultural expansion into forested areas has heightened erosion susceptibility. The soil composition throughout the Swat Valley is dominated by sand, with a decrease in sand content downstream. At Kalam, sand content exceeds 80%, gradually decreasing to 40% near Totakan. The valley is fragmented into smaller valleys and sub-valleys. Soil thickness increases, and sand content decreases on both sides of the Khwar. Texture-based classifications include loamy sand, sandy loam, sandy clay loam, loam, and silt loam. Sandy loam, constituting over 70% of the soil, is prevalent, explaining the low water retention capacity. It is the primary soil type in irrigated land, covering 60%, while rain-fed areas like Rangmala comprise 10%, and irrigated areas constitute 40%. Along the Swat River, a 50 to 300-meter strip on both banks features loamy sand, with higher sand content in foothill villages like Landakai (Ahmad et al., 2015) (Figure 5).

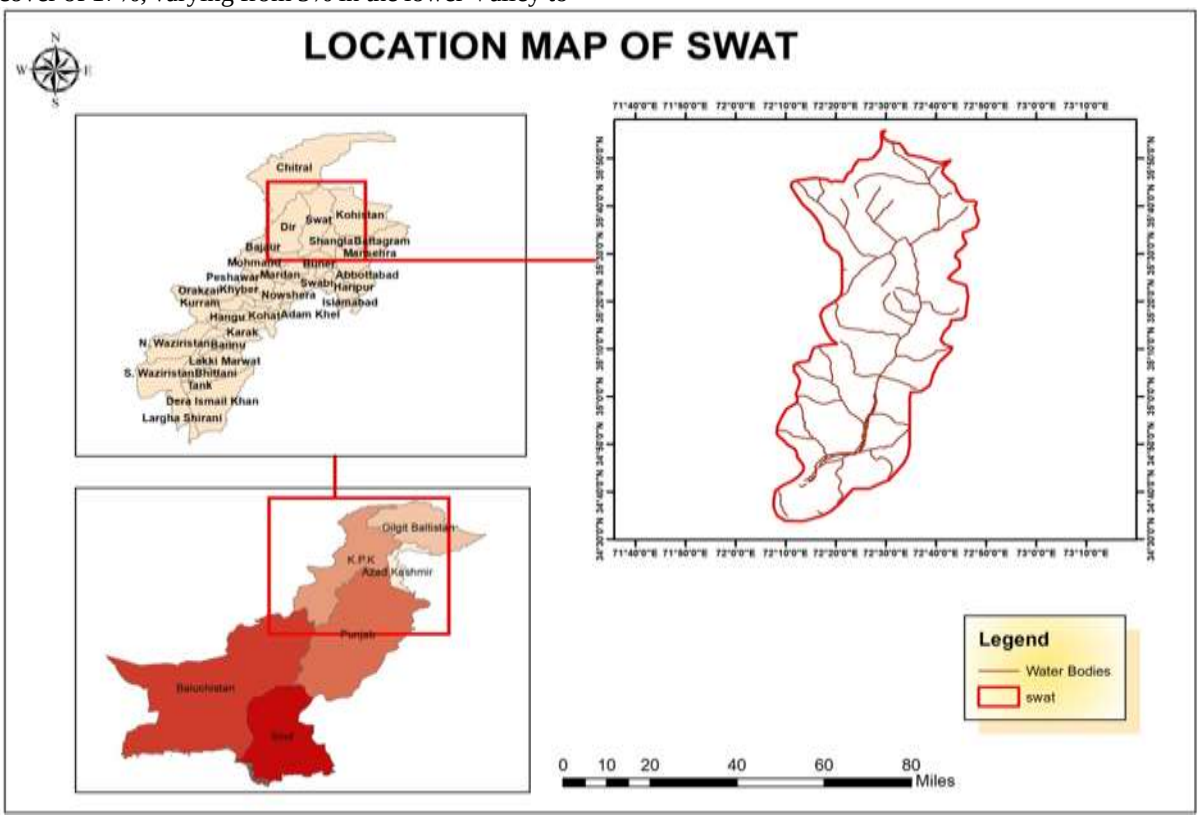

Figure 5: Location Map of SWAT

Soil Slope

In the Swat Valley, spanning 120.36 kilometers from Kalangai to Kalam, the elevation rises from 567 to 2969 meters, with an average gain of 19.96 meters per kilometer. The region can be segmented into three parts, revealing varying average increases: 24 meters per kilometer from Kalam to Fatehpur, 21 meters per kilometer from Fatehpur to Mingora, and 2 meters per kilometer from Mingora to Kalangai. The valley widens to the south and narrows northward, gradually rising elevation. The terrain from Mingora to Kalangai appears level but is vulnerable to erosion due to varying textures. The irrigated and semi-irrigated areas from Mingora through Fatehpur to Kalam are steep, while the rain-fed region from Fatehpur to Kalangai is severely sloping. Gully

erosion poses a risk to floodplain farming. The Matta and Kabal Valleys and the foothills are classified as steep, ranging from 25 to 60 percent slope. Lower Dir is highly sloping, with some plain areas in the middle of valleys, predominantly used for mountain farming on gravel and sandy soil (Table 3).

Table 4: Soil Texture of Selected Sample collected from River Swat

Region(% of total)	Texture classes	No of Sample	Sand% (Average)	Silt% (Average)	Clay% (Average)
Upper Swat (8.96%)	Loamy sand	10	80.70	10.34	8.96
	Sandy loam	9	67.44	20.66	11.90
Middle Swat northern side of Swat River (33.96)	Sandy loam	59	68.06	17.86	14.08
	Sandy clay	2	49.87	13.79	36.34
	Sandy clay loam	9	64.54	13.53	21.94
	Loamy sand	2	83.05	8.68	8.26
Middle Swat southern side of River Swat(30.66)	Sandy clay	2	50.49	13.14	36.37
	Sandy clay loam	6	52.86	23.27	23.87
	Loam	8	44.52	38.67	16.83
	Sandy loam	36	61.43	25.65	12.87
	Loamy sand	5	77.06	16.16	6.78
	Silt loam	8	37.68	62.90	9.43
Lower Swat Northern side of River Swat (11.79%)	Sandy loam	14	61.48	24.88	13.05
	Loam	6	38.90	42.07	19.03
	Sandy clay loam	5	48.69	24.08	27.22
Lower Swat Southern side of River Swat (14.63%)	Sandy clay loam	3	53.31	23.0	23.61
	Silt loam	2	28.87	52.14	19.00
	Sandy loam	14	69.25	28.94	11.80
	Loam	12	45.73	38.43	15.84

Hydrology of Swat River

River Swat's suspended load fluctuates seasonally, varying from 19 to 116 mg/l in low flow (October to March) and 137 to 692 mg/l in high flow (April-September). The estimated average annual suspended load 2004 was 0.855 tonnes/acre/year, rising to 1.628 tons/acre/year with floods. This underscores the need for attention from the Agriculture and Forest Departments to address soil loss, advocating for agronomic methods, afforestation, and agroforestry. The Swat River Basin receives 926 mm average annual rainfall, with March as the wettest month and snowfall contributing 60 percent. Stream flow averages 170 m3/s from 1979 to 2010, with significant seasonal variations, notably during the peak flow season from May to August.

Watershed Delineation

Watershed delineation consists of sub-basins and reaches. It consists of topography, contour slope, and DEM of Swat. DEM is downloaded from USGS. It consists of a projected coordinate system. After adding the DEM set the projected coordinate system (Figure 6).

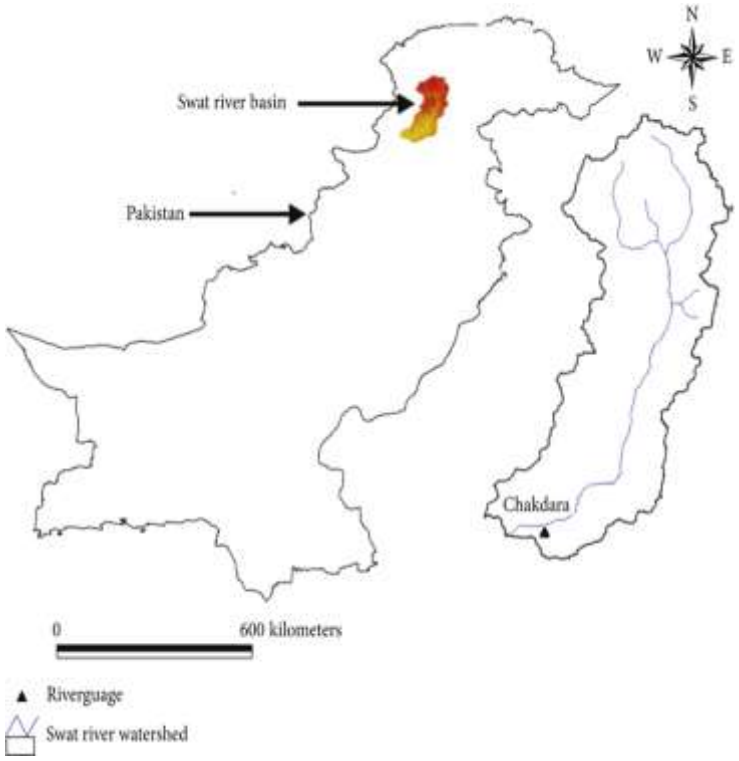

Figure 6: Swat River Basin

Results and Discussion

Model Calibration

The HBV-light model initially had certain tweaks to the parameter ranges (obtained from prior studies), and sampling was carried out using 5000 Monte Carlo runs with a predetermined threshold efficiency. The model was calibrated using a variety of parameter settings that the Monte Carlo runs produced, selecting only those that provided sufficient Nash-Sutcliffe efficiency (NSE). The optimized parameter settings provide the best values of NS efficiency, coefficient of determination (R2), and mean difference between observed and simulated stream flow measurements. Graph no 1 illustrates the observed and simulated discharge for each of the study basin's four outlet stations between 1982 and 2000, one is the final outlet point (Swat River Basin). The observed simulations show that the HBV-light model typically underestimates the peak values while more accurately simulating the low flow period. The average simulated and observed discharges have been seen to be relatively close to one another (Selling, 2015).

The graph shows that the observed and HBV-light simulated discharges behaved similarly. The efficiency numbers and visual examination of the hydrographs show that the HBV-light model performs satisfactorily. Because simulations typically reveal that most precipitation happens under freezing circumstances in the form of snow, the most important parameter for the river basins under consideration is the threshold temperature. On the other hand, the majority of runoff occurs in the summer when the temperature is above freezing (Selling, 2015) (Figures 7 & 8; Tables 4, 5**)**.

Table 4: Summary of Calibration Results

Water Balance (mm/year)	Sub-catchment
Sum Qsim	1291
Sum Qobs	1391
Sum Precipitation	771
Sum AET	216
Sum PET	667
Contribution of Q1	0.728
Contribution of Q2	0.272
Coefficient of determination	0.80
Model efficiency	0.70

Table 5: Performance of the HBV model during calibration

KGE	**0.701**
NSE	0.751
PBIAS	3.2%
R2	0.789

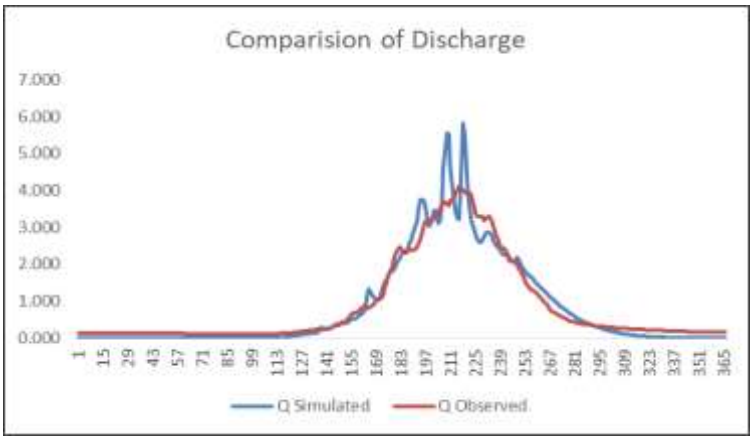

Figure 7: comparison of simulated and observed discharge

Calibration Model Results

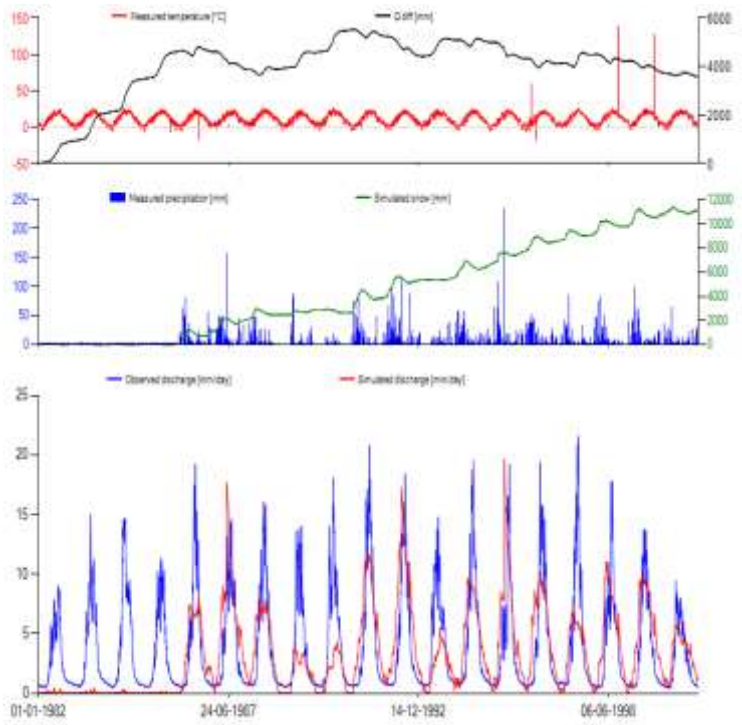

Figure 8: Model Calibration Results

Validation

For the validation period from 1 January 2001 to 31 December 2010, the calibrated parameter sets were utilized to model the catchment behavior using an independent data set. The validation period's efficiency range (0.563 to 0.872) is somewhat improved compared to the calibration period's (Figure 9; Tables 6, 7, 8, 9).

Table 6: Summary of Validation Results

Water Balance (mm/year)	Sub-catchment
Sum Qsim	1200
Sum Qobs	1248
Sum Precipitation	919
Sum AET	449
Sum PET	646
Contribution of Q1	0.351
Contribution of Q2	0.649

Coefficient of determination	0.83
Model efficiency	0.72

Table 7: Performance of the HBV model during Validation

KGE	**0.825**
NSE	0.701
PBIAS	0.05%
R2	0.859

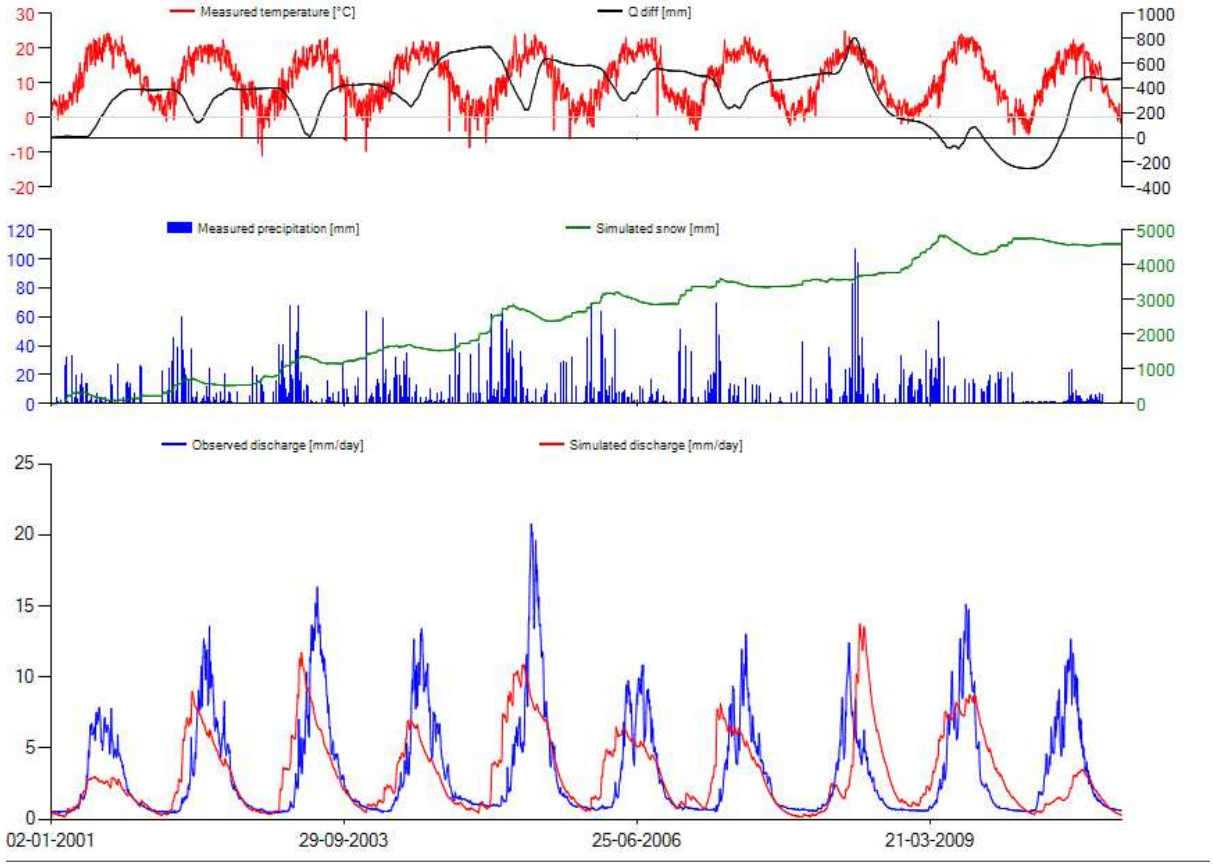

Figure 9: Validation Model Results

Ten year data is used for Validation (2001 to 2010).
These results are showed by HBV-Light model

Table 8: Coefficients for calibration quality assessments, goodness-of-fit measures

Benchmark Description	Definition 1	Value for Perfect-Fit	Range
Coefficient of determination (R2)	$\frac{(\sum(Qobs-\overline{Qobs})(Qsim-\overline{Qsim})2}{\sum(Qobs-\overline{Qobs})2\sum(Qsim-\overline{Qsim})2}$	1	$-\infty$ to 1
Nash–Sutcliffe efficiency (NSE)	$1-\frac{\sum(Qobs-Qsim)2}{\sum((Qobs-\overline{Qobs})2}$	1	$-\infty$ to 1
Efficiency for log(Q)	$1-\frac{\sum(\ln Qobs-\ln Qsim)2}{\sum((\ln Qobs-\overline{\ln Qobs})2}$	1	$-\infty$ to 1
Flow-weighted efficiency	$1-\frac{\sum(Qobs/\overline{Qobs})(Qobs-Qsim)2}{\sum(Qobs/\overline{Qobs})(Qobs-\overline{Qobs})2}$	1	$-\infty$ to 1
Mean difference	$\frac{\sum(Qobs-Qsim)}{n}365$	0	$-\infty$ to ∞
Efficiency for peak flows	$1-\frac{\sum(peakQobs-peakQsim)2}{\sum(peakQobs-\overline{peakQobs})2}$	1	$-\infty$ to 1
Volume error	$1-\frac{1}{n}\sum\frac{\lvert Qobs-Qsim\rvert}{Qobs}$	1	$-\infty$ to 1
MARE measure	$1-\frac{1}{n}\sum\frac{\lvert Qobs-Qsim\rvert}{Qobs}$	1	$-\infty$ to 1

Lindstrom measure	$NSE - 0.1\frac{\lvert\sum(Qobs - Qsim)\rvert}{\sum(Qobs)}$	1	$-\infty$ to 1
Spearman rank	$\frac{\sum(Robs - \overline{Robs})(Ssim - \overline{Ssim})}{\sqrt{\sum(Robs - \overline{Robs})2}\sqrt{\sum(Ssim - \overline{Ssim})2}}$	1	$-\infty$ to 1
The efficiency of low flows	$1 - \frac{\sum(lowQobs - lowQsim)2}{\sum(lowQobs - \overline{lowQobs})2}$	1	$-\infty$ to 1
Low-flow difference	$\sum(lowQobs - lowQsim)$	0	$-\infty$ to ∞

Table 9: List of parameters with their units and description

Parameter Name	Unit 1	Description
PERC	mm/Δt	maximal flow from the upper to the lower box
UZL	mm	threshold parameter
K0	1/Δt	storage (or recession) coefficient 0
K1	1/Δt	storage (or recession) coefficient 1
K2	1/Δt	storage (or recession) coefficient 2
MAXBAS	Δt	routing, length of the triangular weighting function
CET	1/◦C	potential evaporation correction factor
TT	◦C	threshold temperature
CFMAX	mm/Δt	degree–Δt factor
SP	-	seasonal variability in degree–Δt factor
SFCF	-	snowfall correction factor
CFR	-	refreezing coefficient
CWH	-	water-holding capacity
FC	mm	maximum soil moisture storage
LP	-	the threshold for reduction of evaporation (SM/FC)
BETA	-	a parameter that determines the relative contribution to runoff from rain or snowmelt

Precipitation from 1981 to 2010

The graph shows the precipitation trends of Swat River Basin from 1981 to 2010. According to this graph, the highest precipitation occurred from 1990 to 1995, and the lowest precipitation occurred from 1981 to 1985. The data used to plot the graph is taken by Wapda, which shows the peaks and troughs of Precipitation in Swat River (Figure 10)**.**

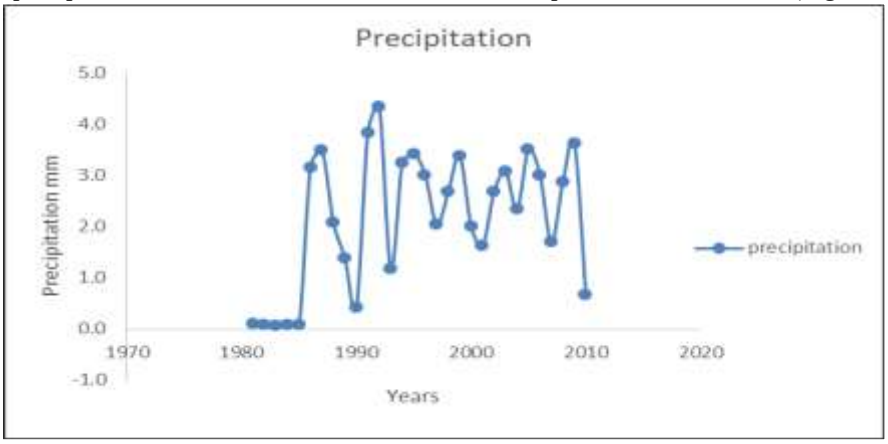

Figure 10: Precipitation of 30 years

Discharge from 1981 to 2010

The following graph shows the discharge of the Swat River Basin from 1981 to 2010. According to the following graph, the highest discharge of the Swat River Basin occurred from 1990 to 1995 and the lowest discharge occurred from 1980 to 1985 (Figure 11).

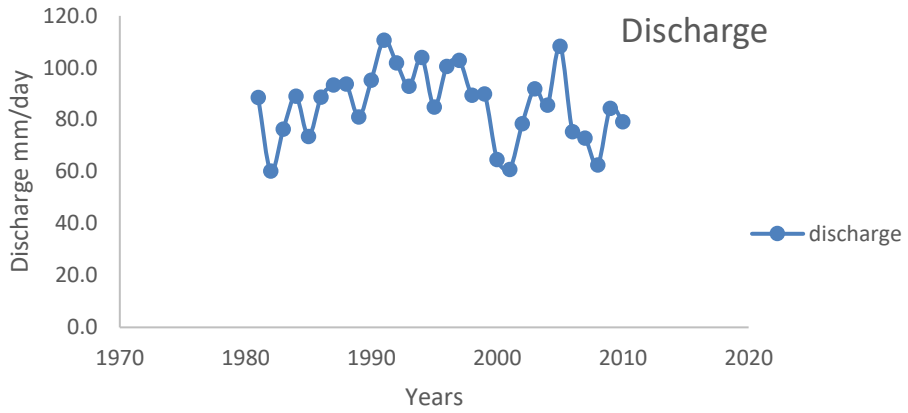

Figure 11: Discharge of Swat River Basin

ET of Swat River Basin

An essential component of the water balance is the Earth's water vapour loss to the atmosphere through direct evaporation and transpiration from vegetation. But there is no straightforward way to measure these elements. This has resulted in several formulae created to estimate direct water loss from meteorological information. **Thorn Thwaite method** is used to calculate ET in research. Several drainage basins' worth of rainfall and runoff data were used to construct the Thorn Thwaite method. The outcome is an empirical link between potential evapotranspiration and mean air temperature. Despite the method's clear limits and intrinsic simplicity, it performs surprisingly effectively. It does not necessarily have the best theoretical foundation or be the most precise procedure. These distinctions, on the other hand, most likely fall under the vapor flux or heat balance techniques. The presumption that there is a strong association between mean temperature and some other important elements, such as radiation, atmospheric moisture, and wind, is one of the more glaring flaws in Thorn Thwaite's empirical relationship (Table 10, Figure 12).

The fundamental formula provided by Thorn Thwaite in the form for calculating monthly potential evapotranspiration

e=1.6 (lOT/I)"

e=monthly potential evapotranspiration (cm.)

T=monthly mean temperature (" C.)

I is the sum of 12 monthly index values.

Where I is a function of the monthly average temperature and is a constant for a given place. (Exponent is an empirically found I function with values of 6.75X 13-7.71X 10-512+1.79X10-2 13.0.49 (Palmer and Havens, 1958).

Table 10: The ET of Swat River Basin

Months	ET
January	0.09
February	0.26
March	0.86
April	1.78
May	2.74
June	3.48
July	3.70
August	3.28
September	2.53
October	1.49
November	0.69
December	0.26

Graphic representation of ET

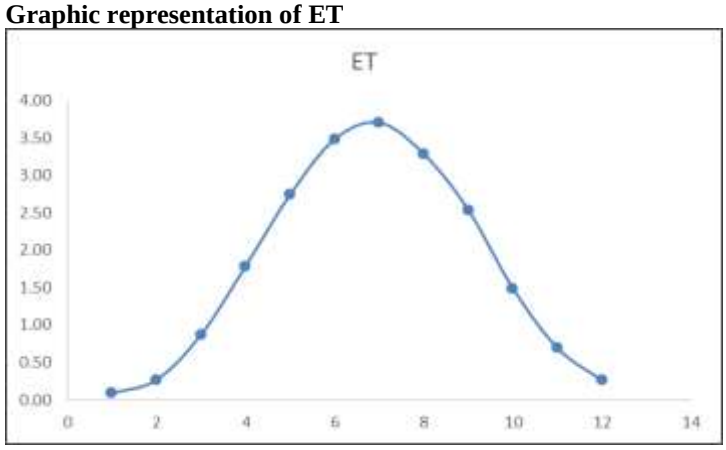

Figure 12: ET of Swat River Basin

Mean Temperature of Swat

Mean temperature is the average air temperature throughout a specific period, typically a day, a month, or a year, as measured by a thermometer that has been properly exposed. The mean temperature is often calculated each month and the entire year for climatological tables. Monthly and daily basis mean of temperature was taken. The daily mean temperature is computed by summing the Maximum and Minimum temperatures, then dividing the result by two. The average monthly temperature is: It is computed by summing the daily means for all of the days in the month and then dividing the result by the number of days in a month. Temperature data for thirty years (1981 to 2010) was collected from WAPDA, including the Maximum and Minimum temperatures of Swat River Basin. This data was sorted by year, and then this data's mean was taken to calculate the ET (Figure 13 & 14; Table 11).

Table 11: The mean temperature of thirty years

Months	Mean Temp
January	1.0

February	2.4
March	6.3
April	11.0
May	15.1
June	18.0
July	19.2
August	18.2
September	15.6
October	10.6
November	5.9
December	2.6

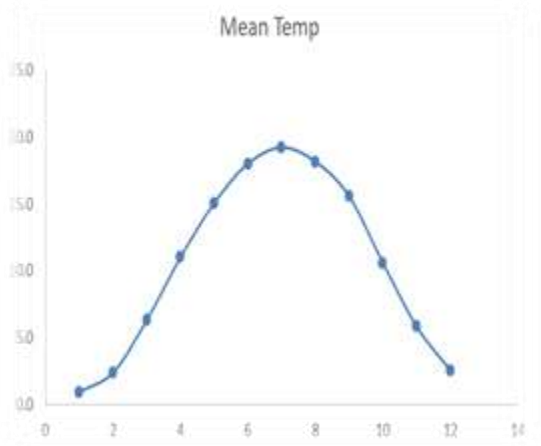

Figure 13: Mean temperature of Thirty years (1981-2010)

Following graph shows the comparison of Evapotranspiration VS Mean temperature of thirty years of Swat River Basin

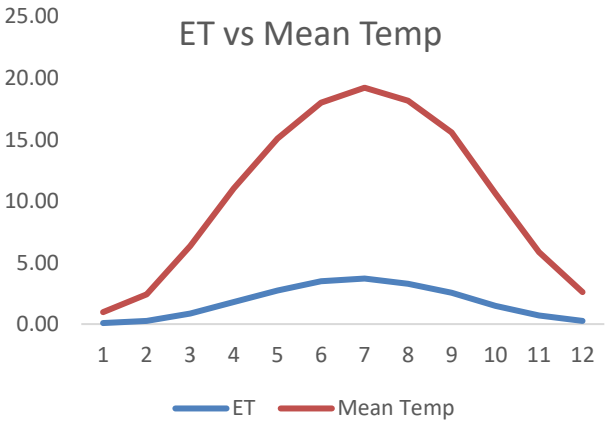

Figure 14: Comparison of ET and Mean Temperature

Conclusions and Recommendations

This study uses the general water balance approach and the HBV-light model to assess snow melt contributions in a snow-covered watershed through rainfall-runoff modeling. The research identifies the HBV-light model's effectiveness in simulating stream flow and snowmelt in a snow-fed basin, displaying satisfactory calibration (1981-2000) and validation (2001-2010) results. Emphasizing the significant impact of parameter set values on model performance, the study underscores the challenge of uncertainty in optimal parameter configuration selection. Sensitivity tests reveal the substantial influence of climate change, particularly temperature increase, on stream flow characteristics. Geographic Information Systems (GIS), especially utilizing digital elevation models, play a crucial role in water resource management, aiding in watershed delineation and basin modeling. The GIS Arc Hydro tool is highlighted for its utility in determining grid directions for catchment areas, drainage lines, and flow accumulation. Recommendations include employing more extensive data to better understand local conditions, utilizing the HBV-Light model for runoff simulation in snow cover catchments, and considering increased time step data for enhanced accuracy in rainfall and discharge analyses.

List of Abbreviations

WAPDA	Water and Power Development Authority
GIS	Geographical information system
MAF	Million acre feet
MM	millimeter
IPCC	intergovernmental panel on climate change
NASA	National Aeronautics and Space Administration

References

Acreman, M. (1999). Water and Ecology Linking the Earth's Ecosystems to its Hydrological Cycle. *Revista CIDOB d'Afers Internacionals*, 129-144. https://www.jstor.org/stable/40586153

Ahmad, H., Öztürk, M., Ahmad, W., and Khan, S. M. (2015). Status of natural resources in the uplands of the Swat Valley Pakistan. *Climate change impacts on high-altitude ecosystems*, 49-98 https://doi.org/10.1007/978-3-319-12859-7_2.

Ahmadi Dehrashid, A., Valizadeh, N., Gholizadeh, M. H., Ahmadi Dehrashid, H., and Nasrollahizadeh, B. (2022). Perspectives of Climate Change. *In* "Climate Change: The Social and Scientific Construct", pp. 369-388. Springer https://doi.org/10.1007/978-3-319-12859-7_2.

Ahmed, S. I. Transboundary River Water Management in South Asia: A Study of Indus Basin.

Ali, A. F., Xiao, C.-d., Zhang, X.-p., Adnan, M., Iqbal, M., and Khan, G. (2018). Projection of future streamflow of the Hunza River Basin, Karakoram Range (Pakistan) using HBV hydrological model. *Journal of Mountain Science* **15**, 2218-2235. https://doi.org/10.15244/pjoes/66719

Anjum, M. N., Ding, Y., Shangguan, D., Ijaz, M. W., and Zhang, S. (2016). Evaluation of high-resolution satellite-based real-time and post-real-time precipitation estimates during 2010 extreme flood event in Swat River Basin, Hindukush region. *Advances in Meteorology* **2016**. https://doi.org/10.1155/2016/2604980

Ashraf, A., Roohi, R., Naz, R., and Mustafa, N. (2014). Monitoring cryosphere and associated flood hazards in high mountain ranges of Pakistan using remote sensing technique. *Natural hazards* **73**, 933-949 https://doi.org/10.1007/s11069-014-1126-3.

Bhattarai, S., Zhou, Y., Shakya, N. M., and Zhao, C. (2018). Hydrological modelling and climate change impact assessment using HBV light model: a case study of Narayani River Basin, Nepal. *Nature Environment and Pollution Technology* **17**, 691-702 https://doi.org/10.1016/j.jhydrol.2008.03.015.

Bizuneh, B. B., Moges, M. A., Sinshaw, B. G., and Kerebih, M. S. (2021). SWAT and HBV models' response to streamflow estimation in the upper Blue Nile Basin, Ethiopia. *Water-Energy Nexus* **4**, 41-53. https://doi.org/10.1016/j.wen.2021.03.001

Bouadila, A., Tzoraki, O., and Benaabidate, L. (2020). Hydrological modeling of three rivers under Mediterranean climate in Chile, Greece, and Morocco: study of high flow trends by indicator calculation. *Arabian Journal of Geosciences* **13**, 1-17. https://doi.org/10.1007/s12517-020-06013-2

Dawood, M., Rahman, A.-u., Mahmood, S., Rahman, G., and Nazir, S. (2021). Assessing the impact of climatic change on discharge in Swat river basin using fuzzy logic model. *Arabian Journal of Geosciences* **14**, 1850. https://doi.org/10.1007/s12517-021-08219-4

Habib, Z. (2004). Scope for reallocation of river waters for agriculture in the Indus Basin. *École nationale du génie rural, des eaux et des forêts*. https://doi.org/10.3390/su13095303

Hanna, K. C., Hanna, K. C., and Culpepper, R. B. (1998). "GIS and site design: New tools for design professionals," John Wiley & Sons. https://doi.org/10.1007/s101090050027

Kaur, S. Global Warming: A Visible Threat the Social and Physical Impacts of Climate Change. *www. excelpublish. com*, **195**. https://doi.org/10.3390/su9020293

Khan, S. U., Hassan, M., Khan, F., and Bari, A. (2010). Climate classification of Pakistan. Balwois Ohrid. https://doi.org/10.3390/land10101026

Khorchani, N. (2016). Modelling the impact of land use changes on hydrology using HBV-light. http://repository.pauwes-cop.net/handle/1/99

Macauley, D. (2010). "Elemental philosophy: Earth, air, fire, and water as environmental ideas," State University of New York Press. https://doi.org/10.3390/fire6020079

Malik, M., and Ashraf, M. (2021). Hydro-Morphology of the Tributaries and Active Flood Plains of the River Indus. *Pakistan Council of Research in Water Resources (PCRWR)*, **80** https://doi.org/10.3390/w14192984.

McCuen, R. H., Knight, Z., and Cutter, A. G. (2006). Evaluation of the Nash–Sutcliffe efficiency index. *Journal of hydrologic engineering* **11**, 597-602. https://doi.org/10.1061/(ASCE)1084-0699(2006)11:6(597

Mishra, R. K. (2023). Fresh water availability and its global challenge. *British Journal of Multidisciplinary and Advanced Studies* **4**, 1-78 https://doi.org/10.1061/(ASCE)1084-0699(2006)11:6(597).

Molden, D. (2013). "Water for food water for life: A comprehensive assessment of water management in agriculture," Routledge. https://doi.org/10.1029/2020WR029001

Moriasi, D. N., Gitau, M. W., Pai, N., and Daggupati, P. (2015). Hydrologic and water quality models: Performance measures and evaluation criteria. *Transactions of the ASABE* **58**, 1763-1785. (doi: 10.13031/trans.58.10715

Nonki, R. M., Lenouo, A., Tshimanga, R. M., Donfack, F. C., and Tchawoua, C. (2021). Performance assessment and uncertainty prediction of a daily time-step HBV-Light rainfall-runoff model for the Upper Benue River Basin, Northern Cameroon. *Journal of Hydrology: Regional Studies* **36**, 100849. https://doi.org/10.1016/j.ejrh.2021.100849

Palmer, W. C., and Havens, A. V. (1958). A graphical technique for determining evapotranspiration by the Thornthwaite method. *Monthly Weather Review* **86**, 123-128 https://doi.org/10.1007/BF00868097.

Selling, B. (2015). Modelling Hydrological Impacts of Forest Clearcutting through Parameter Regionalization. urn:nbn:se:uu:diva-267402

Singh, G. (2017). Sustainable groundwater management in India-challenges and prospects. *Indian Journal of Economics and Development* **13**, 721-727. Singh, G. (2017). Sustainable groundwater management in India-challenges and prospects. Indian Journal of Economics and Development 13, 721-727.

Soundharajan, B.-S., Adeloye, A. J., and Remesan, R. (2016). Evaluating the variability in surface water reservoir planning characteristics during climate change impacts assessment. *Journal of Hydrology* **538**, 625-639. https://doi.org/10.1016/j.jhydrol.2016.04.051

Vainu, M., Terasmaa, J., and Häelm, M. (2015). Relations between groundwater flow in an unconfined aquifer and seepage patterns in a closed-basin lake in glacial terrain. *Hydrology Research* **46**, 325-342. https://doi.org/10.1007/978-3-319-12859-7_2

Declarations

Acknowledgments

Not applicable

Funding

Not applicable

Author's contributions

AI collected the literature and wrote the manuscript. WA and RN edit the manuscript in original. All authors have read and approved the final manuscript.

Ethics approval and consent to participate

Not applicable

Consent for Publication

Not applicable

Competing interests

The authors declare that they have no competing interests.